

Offshore infrastructure planning using a vine copula approach for environmental conditions

an application for replacement maintenance of tidal energy infrastructure

de Nie, Ruben; Leontaris, Georgios; Hoogendoorn, Don; Wolfert, A. R.M.(Rogier)

DOI

[10.1080/15732479.2018.1558268](https://doi.org/10.1080/15732479.2018.1558268)

Publication date

2019

Document Version

Accepted author manuscript

Published in

Structure and Infrastructure Engineering

Citation (APA)

de Nie, R., Leontaris, G., Hoogendoorn, D., & Wolfert, A. R. M. (2019). Offshore infrastructure planning using a vine copula approach for environmental conditions: an application for replacement maintenance of tidal energy infrastructure. *Structure and Infrastructure Engineering*, 15(5), 600-617.
<https://doi.org/10.1080/15732479.2018.1558268>

Important note

To cite this publication, please use the final published version (if applicable).
Please check the document version above.

Copyright

Other than for strictly personal use, it is not permitted to download, forward or distribute the text or part of it, without the consent of the author(s) and/or copyright holder(s), unless the work is under an open content license such as Creative Commons.

Takedown policy

Please contact us and provide details if you believe this document breaches copyrights.
We will remove access to the work immediately and investigate your claim.

Offshore infrastructure planning using a vine copula approach for environmental conditions

An application for replacement maintenance of tidal energy infrastructure

Ruben de Nie^a, Georgios Leontaris^b, Don Hoogendoorn^a, A.R.M. (Rogier) Wolfert^b

^aResearch & Development, Damen Shipyards, The Netherlands;

^bInfrastructure Design and Management, Fac. Civil Engineering and Geosciences, TU Delft, The Netherlands

ARTICLE HISTORY

Compiled November 16, 2018

ABSTRACT

Installation and maintenance operations of offshore assets are impacted by local environmental conditions such as wave height and period, wind speed and current velocity. These parameters are substantially of influence for the asset planning (time and costs) given the uncertainty of operational windows. In this article, a method is proposed to construct realistic time series of the aforementioned dependent conditions using a vine copulas approach. This method makes it possible to obtain a large number of realizations of these conditions at a certain location. It is shown that the operational windows remain persistent with the original limited dataset. Moreover, this method enables the incorporation of environmental uncertainties in the operational planning processes. To illustrate the value of this method, an application regarding replacement maintenance of a tidal energy infrastructure is examined. For this purpose, the maintenance activities are represented as a semi-Markov decision process. For every synthetic environmental time series, the algorithm finds the optimal set of decisions and the corresponding maintenance plans, including replacement costs and revenue losses. It is shown that the proposed method is effective in replacement maintenance decision making, while taking into account the environmental uncertainties.

KEYWORDS

Offshore energy infrastructure; Uncertain operational windows; Vine copulas; Environmental time series; Probabilistic planning; Tidal Energy Converter; Replacement maintenance

1. Introduction

To address the steadily increasing energy demand worldwide (U.S. Energy Information Administration, 2017), offshore infrastructure for the extraction of oil and natural gas are usually required. Moreover, over the last years, due to the depletion of fossil fuels, the development of technologies which harness renewable energy sources has

flourished (Ellabban, Abu-Rub, & Blaabjerg, 2014). Several promising technologies among these are also located offshore (International Renewable Energy Agency, 2014). Some examples are offshore wind energy, offshore wave and tidal energy and recent offshore developments such as floating solar panels (Patil (Desai) Sujay, Wagh, & Shinde, 2017).

It is a fact that there are significant differences between the aforementioned technologies. Oil and gas technologies are well established, offshore wind energy is approaching maturity while one could argue that the others are still in early development stage. However, all of these offshore energy generating technologies have one common characteristic. The required installation and or maintenance operations are very much dependent on the local environmental conditions: i.e., wave, wind and tidal conditions, which will impact these operations severely with significant financial impacts on both the operational expenditures and the work schedules.

The environmental conditions that usually hinder the majority of the offshore operations concern stochastic variables such as wind speed, wave height and wave period. The wind and wave influence on the uncertainty of the operational window (i.e., the period in which offshore works can be executed) is a well-known problem and has been extensively studied for installation and maintenance activities of offshore wind farms (Stålhane, Vefsnmo, Halvorsen-Weare, Hvattum, & Nonås, 2016; Kikuchi et al., 2009; Martin, Lazakis, Barbouchi, & Johanning, 2015; Leontaris, Morales-Nápoles, & Wolfert, 2016). Probabilistic models have been developed to cope with uncertainties of the duration of the operational windows and its effect on offshore infrastructural assets planning (time and costs).

However, offshore infrastructure operations often also require subsea activities such as installation of submarine cables or pipes and drilling support of oil and gas industry. These operations often require Remote Operated Vehicles (ROVs: tethered underwater mobile devices) which besides wind and wave, are also stalled by the velocity of currents. Furthermore, in tidal energy infrastructures, consisting of Tidal Energy Converters (TECs), the fast flowing currents impact the economic efficiency of the assets in direct relation with the limitation for performing (corrective) maintenance activities. Station-keeping capabilities of the maintenance vessel are generally not sufficient to perform an on-site replacement operation. The recurring character of the tidal current further reduces the possibility of extensive operational windows. Hence, the combination of the tidal current, waves and wind limits offshore infrastructure operational processes drastically.

Therefore, in this article a method is proposed to make use of vine copulas for describing the dependence between the aforementioned environmental variables, including the current velocity, and generating time series. Copulas theory has been used in numerous studies over the past few years. Some of these studies also focus on infrastructure engineering applications: e.g., design optimisation of different infrastructural assets (Attoh-Okine, 2013; Liu, Wu, Zhang, & Wang, 2017), reliability engineering of geotechnical structures (Li, Phoon, Wu, Chen, & Zhou, 2013; Tang, Li, Rong, Phoon, & Zhou, 2013) and modelling of flood risk (Masina, Lamberti, & Archetti, 2015; Joyce, Chang, Harji, & Ruppert, 2018). The main reason for the application of copula theory in a variety of applications is that this allows the construction of joint distributions of variables using their marginal probability distributions and measures of dependence, achieving the description of dependence among multivariate data (Clemen & Reilly, 1999; Tang, Li, Zhou, & Phoon, 2015). Moreover, this approach makes it possible to

investigate and to describe asymmetries in the joint distributions because there are families of copulas which satisfy different tail behaviour (Joe, 2015). In this article, proper description of these asymmetries and especially that of the upper tail dependence is crucial for offshore operations because these are mainly influenced by extreme environmental conditions. Previous studies on the application of vine copulas for describing sea states have already showed the relevance of modelling the dependence between wind and wave conditions (Montes-Iturrizaga & Heredia-Zavoni, 2016; Leonardis et al., 2016; Jäger & Nápoles, 2017). This article extends these studies including the tidal velocity as an extra important environmental condition parameter.

Lastly, it is worth mentioning that other methods were also used to represent the environmental conditions, such as creating a full numerical model for the location of interest (e.g., at EMEC's tidal testing site, see (Lawrence, Kofoed-Hansen, & Chevalier, 2009)). However, developing these types of numerical models requires accurate information for long periods of observation to determine the boundary conditions. Moreover, it is computationally heavy to run the required simulations. Consequently, the complexity of the problem could be reduced by following the method proposed in this article.

2. Vine copulas: theory and application

2.1. Theoretical background

The first publication on copulas was by (Sklar, 1959), who developed a theorem which states that the joint distribution of random variables can be described by their marginal distributions and a copula that describes their dependence structure. Hence, copulas are functions that couple multivariate distribution functions to their one-dimensional marginal distributions. These marginal distributions are uniformly distributed in the range of $[0,1]$ (Genest & Favre, 2007). The use of copulas enables studying the dependence structure of multivariate distributions by means of decoupling the marginal properties of the random variables and the dependence structures.

Indepth studies on copula dependence modeling (Joe, 2015; Aas & Berg, 2009) have compared the set of available copula construction methods which can be placed into two distinct groups, constructions which are described by multivariate copulas and those which can also fully describe the overall dependence by using bivariate copulas. Initially, Joe (Joe, 1996) gave a probabilistic construction of multivariate distributions functions based on simple building blocks called pair-copulas, which model multivariate data sets by using a cascade of lower-dimensional bivariate copulas. Bedford and Cooke (Bedford & Cooke, 2001, 2002) organized these constructions in a graphical way called regular vines. A detailed description of the components is described in (Aas, Czado, Frigessi, & Bakken, 2009). Fitting a Canonical vine might be advantageous when a particular variable is known to be a key variable that governs the interactions between the variables in the data set. In such a situation one may decide to locate this variable at the root of the Canonical vine. On the other hand, the D-vine is mostly preferred if no key variable can be identified in the data and the bivariate combinations have a more or less equal level of dependence. A formal description of the density of an n -dimensional distribution for a C-vine and D-vine is given in (Bedford & Cooke, 2001).

Whilst the base level copula parameters of the vine are directly derived from the input variates, the higher level copulas require the use of the so-called h-function to determine its parameter. The h-function is thus defined as the conditional distribution function of a bivariate copula. In (Joe, 1996) the following relation is derived (under certain regularity conditions) and given that v is univariate,

$$F_{u|v} = \frac{\partial C_{u,v}}{\partial F_v} \quad (1)$$

and when u and v are uniform, this is defined as the h-function (Aas et al., 2009).

$$h(u, v, \theta) = F_{u|v} = \frac{\partial C_{u,v}(ux, v, \theta)}{\partial v} \quad (2)$$

In Equation (2), θ is the set of parameters for the current copula, and the second parameter of $h(\cdot)$ is the conditioning variable. The inverse of the h-function is defined as $h^{-1}(u, v, \theta) = F_{u|v}^{-1}$, which is as the inverse of $h(u, v, \theta)$ with respect to u . The inverse h-function is required when simulating from a vine construction.

Thus, to determine the parametric shapes of the vines one could use the following procedure (Aas et al., 2009):

- Step 1** Select the base level factorisation of the D-vine, based on the highest rank correlation combinations.
- Step 2** Determine which copula families to use at level 1 by plotting the observations, and/or applying a Goodness-of-Fit test (Huang & Prokhorov, 2014; Genest, Quessy, & Rémillard, 2006).
- Step 3** Estimate the parameters of the selected copulas.
- Step 4** Determine the observations required for level 2 as the partial derivatives, using the h-function (eq. 2) of the copulas from level 1.
- Step 5** Determine which copula families to use at level 2 in the same way as at level 1.
- Step ..** Repeat Steps 1-3 for all levels of the construction.

Once the vine has been constructed and all copula families and their respective parameters has been selected, it is possible to simulate new samples. This simulation method is applied to generate synthetic time series which are based on the original environmental measurement data. Figure 1 visualizes a single simulation loop of a D-vine with 4 variables, producing four variates, including the multivariate dependence. The individual nodes are labeled as $v(i, j)$ to correspond with the mathematical simulation algorithm, as is described in (Aas et al., 2009). It should be noted that using vine copulas to simulate synthetic time series requires the input dataset to be time independent and identically distributed (Aas et al., 2009; Nævestad, 2009; Montes-Iturrizaga & Heredia-Zavoni, 2016), since each set of samples is generated independently from previous simulations.

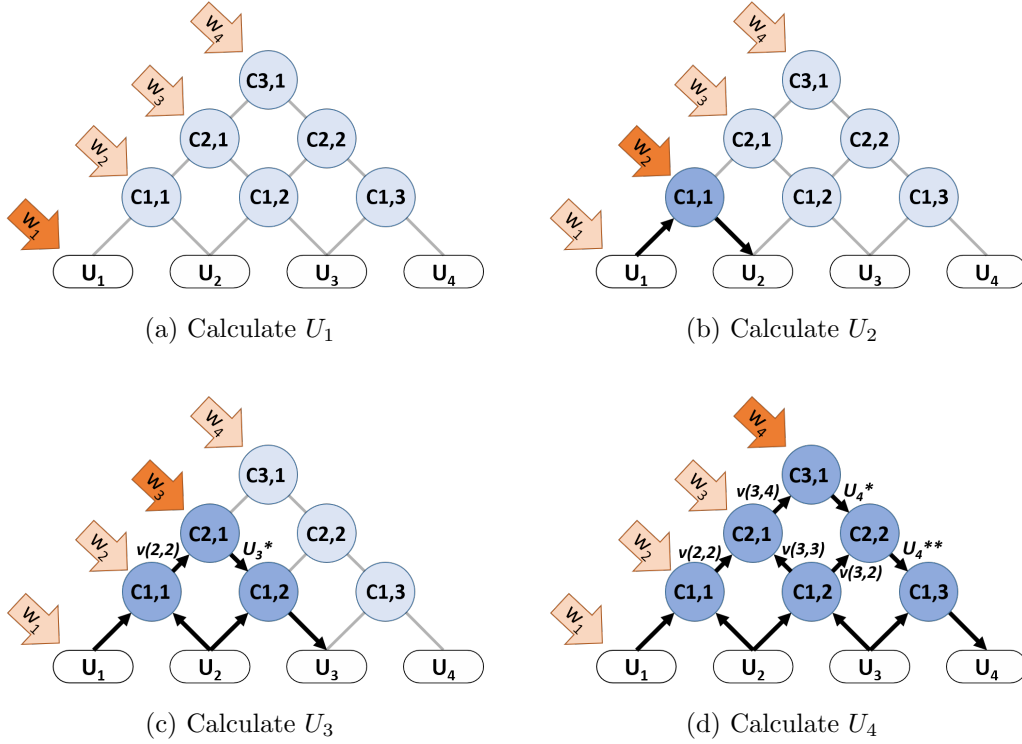


Figure 1. Visualisation of D-vine simulation for one sample set

2.2. Developed simulation algorithm

In an offshore application regarding tidal infrastructure, due to the diurnal recurring character of the tidal currents, the required time interval between time samples has shown to be too small to obtain the aforementioned time independence. Hence, the previously presented procedure can not be directly applied to generate synthetic time series which represent the dependence between the environmental variables as well as their time dependence. It is to the authors' best beliefs that the vine copula theories have in fact not, or very limited, been applied for describing both types of dependence by means of an algorithm. So the following approach is proposed to realistically model the environmental conditions including uncertainty.

First, the simulation process is presented to construct time series for a single variable with a time dependence similar to the original time series. This univariate time series simulation process is as follows:

- Step 1** Build the D-vine by using N lagged sets of the univariate time series ($N = 3$ in Figure 2).
- Step 2** Simulate the full D-vine once using the method described in section 2.1 (Figure 2a).
- Step 3** Shift all generated variates and D-vine parameters one time lag (Figure 2b).
- Step 4** Simulate a new sample using only one random input and the shifted vine parameters (Figure 2c).
- Step 5** Repeat Steps 3 and 4 T_{sim} times to generate the full set of samples in the $[0,1]$ range.

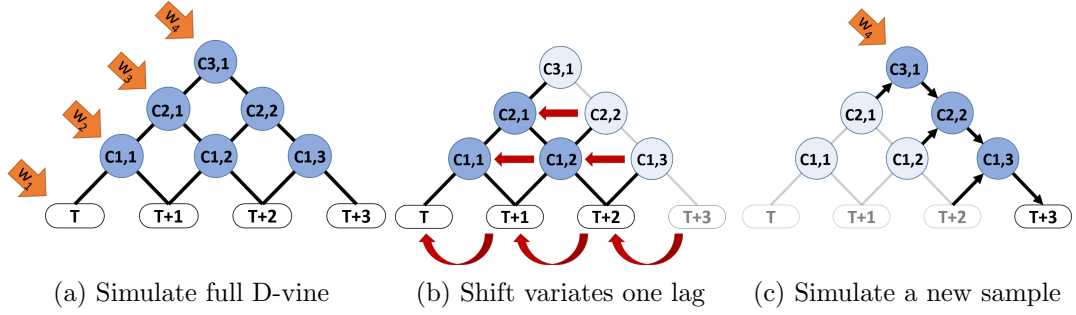


Figure 2. Sampling algorithm for univariate time series

Step 6 Transform the samples back to real values using the empirical distributions of each variable.

By plugging lagged versions of the original univariate time series into the D-vine, the copulas in the vine are used to describe the time dependence between the lags. Simulation of a new sample, as seen in Figure 2c, includes the identified time dependence between the included lags and thus the persistence of the sea state can be modelled. The final step for an accurate representation of the environmental conditions is to expand the simulation method to also describe multivariate dependence between the environmental variables. This requires the univariate dependence of individual variables to be combined by one more vine copula structure.

In this study a special case arises for implementing the current velocity. The magnitude and occurrence in time of V_{curr} does not depend on random processes and can to a high accuracy already be predicted, based on the major driving forces behind it, namely the Earth's rotation and the influence of the sun and moon. Therefore, to preserve the consistency of the recurring tidal velocity profile, it is decided that the synthetic time series of this variable will not be simulated using the D-vine. Alternatively, the entire V_{curr} time series will be copied from the existing dataset and plugged into the D-vine for each time step, using a randomly selected starting point in the original time series. Figure 3 shows how the range is determined in which the starting point is randomly selected. This ensures that the sinusoidal character of the current velocity is maintained and the current velocity acts as the simulation input for the other environmental variables in the D-vine.

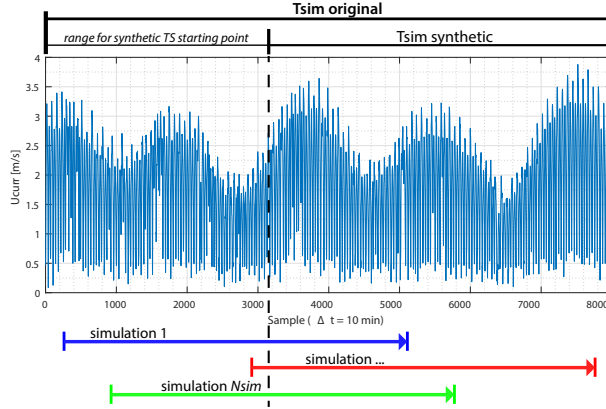


Figure 3. Copying a fraction of the original V_{curr} time series

Hence, the proposed method (*'Univariate time dependence ($\times 3$) \rightarrow Multivariate dependence'*) works as follows. First, it starts with using random numbers to simulate from each of the three univariate D-vines. This creates three independent synthetic time series (excluding V_{curr}), which are then plugged into the multivariate D-vine as w_2, w_3, w_4 input, sample per sample. The variable w_1 is plugged by the samples of the V_{curr} dataset. Finally, the time series which have been generated by the multivariate D-vine are the final output of this approach and describe the environmental time series (H_s, T_p, V_{curr} and V_{wind}), which contain both time dependence and multivariate dependence.

3. Construction of environmental time series for a given location

3.1. Observed locations

The environmental measurements from two fast flowing offshore locations, the Fundy Ocean Research Center for Energy (FORCE) and European Marine Energy Centre (EMEC) tidal field, are used to demonstrate how synthetic time series can be generated by using vine copulas. Whilst both locations are characterized by a high current velocity, the bathymetry and sea state are different. The results from the FORCE data set are presented in this section, whilst the EMEC results can be found in Appendix A.

FORCE's tidal location at the Minas Passage, Canada, has two sensors which have been logging environmental data (Ocean Networks Canada, 2017). A bottom-founded Acoustic Wave and Current (AWAC) is used to log the wave and current data and a meteorological (MET) station measures the wind speed. The AWAC is located at the position of the red dot in Figure 4.

The synchronized measurement datasets for both locations consist of 874 samples with a one hour interval, which describes a 36 days period during the Spring season. No additional data was available for this research, so the seasonality of the environmental conditions could not be observed. It is therefore important to state that the dependence

¹Source: Google Maps

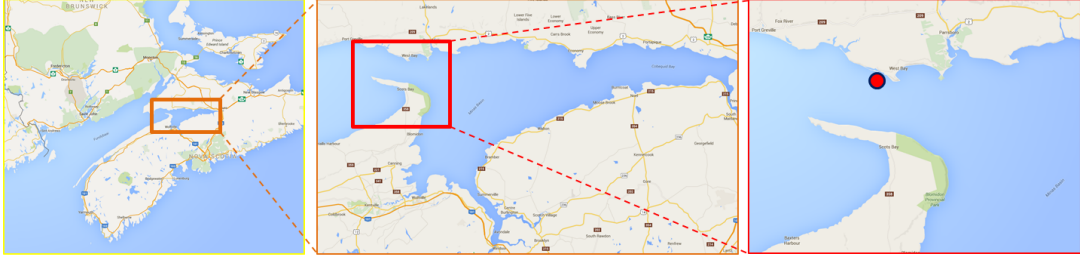


Figure 4. Geographical location of FORCE¹

results in this article cannot be extrapolated for long-term yearly statistics without additional research on the effects of seasonality. However, in case more data become available in the future, the proposed methodology can be used to produce synthetic time series including the seasonality.

3.2. Bivariate dependence

The first step in constructing the vine is determining the factorisation of the variables at the base level. This is done by calculating the Kendall's Tau rank correlation and connecting the strongest bivariate pairs to function as the vine's base. The calculated Kendall rank correlations, regarding FORCE data set, can be found in Table 1. A value of rank correlation equal to zero implies full independence while values equal to +1 or -1 imply full positive and negative dependence respectively.

Table 1. Kendall's Tau rank correlations of FORCE data

	V_{wind}	H_s	T_p	V_{curr}
V_{wind}	1.000	0.292	0.062	0.060
H_s	0.292	1.000	0.229	0.196
T_p	0.062	0.229	1.000	0.393
V_{curr}	0.060	0.196	0.393	1.000

Having performed several analyses on the available environmental datasets, it can be observed that no single key variable is present. Hence, it can be concluded that a D-vine is most suitable for representing the multivariate dependence at the tidal locations. Therefore this article limits itself to using D-vines exclusively.

It should be noted that the the identified bivariate dependence is significantly lower than existing research results (Montes-Iturrizaga & Heredia-Zavoni, 2016), which analyses dependence between H_s, T_p and V_{wind} at sea. This difference can be explained due to the following reasons:

- (1) The tidal locations are geographically different than the location of the reference study. The values from the reference study correspond to the open sea, where the wind is prevalent as the driving force. As is seen in Figure 4, the wind fetch is very limited and it can thus be assumed that wind-driven waves are less occurring at the shallow water tidal location:

- (2) The inclusion of the high current velocities as an additional environmental driving force, besides the wind, creates a different situation in which the waves are not exclusively wind-driven at the tidal location. As these current forces will never occur at open water locations, it does give a possible explanation why the bivariate dependence does not correspond well.
- (3) In (Montes-Iturrizaga & Heredia-Zavoni, 2016) multi-year datasets are used. During these years, differences due to seasonality as well as extreme environmental conditions are observed. The tidal locations are only described by short-term measurement data and therefore do not contain extreme weather events, in which a stronger (upper tail) dependence can possibly be observed.

3.3. Base level factorisation

The four variables have to be factorized in such way that the highest Kendall Tau rank correlation pairs are observed at the base level. An effective method is proposed in this article, which maximizes the sum of the absolute Tau values of the three bivariate pairs. The result of choosing the optimal factorisation pairs from the FORCE dataset are listed in Table 2, using the notation of Figure 1.

Table 2. Base level factorisation of FORCE data

	U_1	U_2	U_3	U_4
FORCE	V_{curr}	T_p	H_s	V_{wind}

3.4. Copula selection

Once the factorisation is known it is possible to determine which copula families best describe the three pairs of bivariate dependence at the base level. There are different bivariate copula types available, depending on the dependence between the variables. In this article, five popular Archimedean and Elliptical one-parameter bivariate copulas were considered to be able to represent cases of upper, lower and no tail dependence (Nelsen, 2006; Embrechts, Lindskog, & Mcneil, 2003; Sibuya, 1960). These copulas are the Clayton, Frank, Gumbel, Gaussian and Student-t and are visualized in Figure 5.

To determine the best fitting copula, first the processed measurement data need to be converted to its corresponding pseudo-observations, defined as normalized ranks, in order to enable the representation using copulas. The method has been performed in this study by using the "VineCopula" package (Schepsmeier et al., 2016) from the "R" software (R Core Team, 2016). The resulting pseudo-observations plots are depicted in Figure 6.

The visual inspection of the pseudo-observations already gave a hint about which copula families best describe the dependence of the three pairs. Still, to ensure the best fitting copula family is selected, a Goodness-of-Fit (GoF) test is conducted which determines the best fit using the AIC (Akaike, 1973) and BIC (Schwarz, 1978). In this research the standard functions of the "VineCopula" (Schepsmeier et al., 2016)

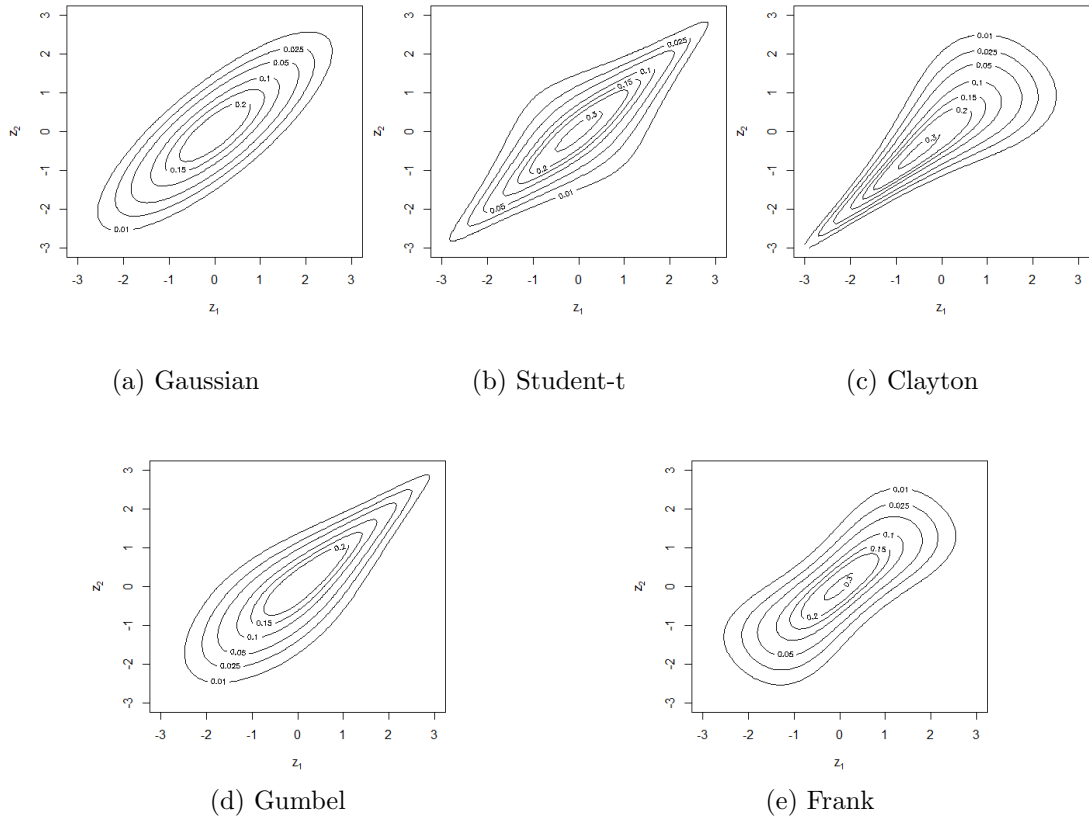


Figure 5. Contour plots of copulas with standard normal marginals ($\tau = 0.60$)

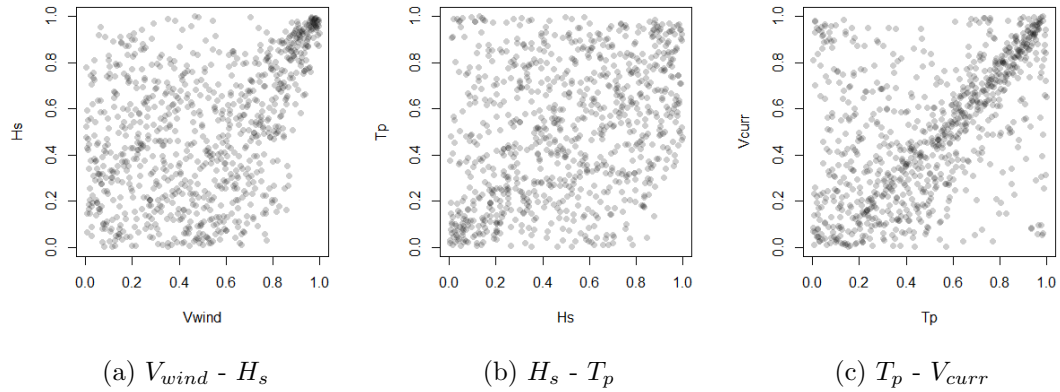


Figure 6. Scatter plots of FORCE pseudo-observations

package are used for this purpose. The best fitting copulas for the bivariate pairs are listed in the rightmost column of Table 3.

The semi-correlations of the bivariate pairs are also analysed, as this is an effective measure to validate the choice of copulas based on the presence of tail dependence. It concerns the calculation of Pearson correlation for the upper-right and lower-left

quadrant which are transformed to the standard normal (Joe, 2015). The calculated upper and lower semi-correlations (of the standard normal scores Z_a and Z_b of two random variables a and b) are defined as: $\rho_{ne} = Cor[Z_a, Z_b | Z_a > 0, Z_b > 0]$ and $\rho_{sw} = Cor[Z_a, Z_b | Z_a < 0, Z_b < 0]$. It can be observed in Table 3 that the calculated best fitting copulas correspond to the outcome of the semi-correlation analysis, as the tail dependence properties fully match.

Table 3. Semi-correlations and selected copula factorisation (FORCE)

Data set	ρ_{sw}	ρ_{total}	ρ_{ne}	Tail dependence	Copula
$V_{wind} - H_s$	-0.158	0.415	0.648	Upper	Gumbel
$H_s - T_p$	0.358	0.329	0.053	Lower	Clayton
$T_p - V_{curr}$	0.289	0.503	0.658	Upper	Gumbel

3.5. Synthetic time series validation

For the purpose of validation of the synthetic time series that were constructed using the 'Univariate time dependence ($\times 3$) \rightarrow Multivariate dependence' method, two comparisons were performed. First, the Kendall's tau correlation coefficient of the synthetic time series were compared to those of the original dataset and secondly the persistence of the operational windows in both cases was examined.

The values of Kendall's tau rank correlation coefficient for one simulation of the FORCE data is presented in Table 4 and shows good correspondence with the rank correlation of the original time series, noted in Table 1. Thus, this is the first indication that the synthetic time series represent the dependence observed in the original data set.

Table 4. Kendall's Tau rank correlations of one FORCE synthetic time series realization

	V_{wind}	H_s	T_p	V_{curr}
V_{wind}	1.000	0.314	0.101	0.059
H_s	0.314	1.000	0.344	0.229
T_p	0.101	0.344	1.000	0.355
V_{curr}	0.059	0.229	0.355	1.000

To further investigate whether or not the produced synthetic time series are realistic, more tests were performed. First, a visual comparison between the synthetic time series and the original dataset was performed. Figure 7 presents the results of this comparison. It can be seen that the synthetic times series present a behaviour similar to the original dataset. Please note, that the values concerning the current velocity have been excluded from this comparison because the initial dataset was used, as explained in section 4.2, resulting in identical time series.

Furthermore, statistical measures such as the mean and the standard deviation for 1000 synthetic time series were calculated and compared to those of the original

dataset for every environmental variable. Table 5 presents these measures. It can be seen that these measures present insignificant differences.

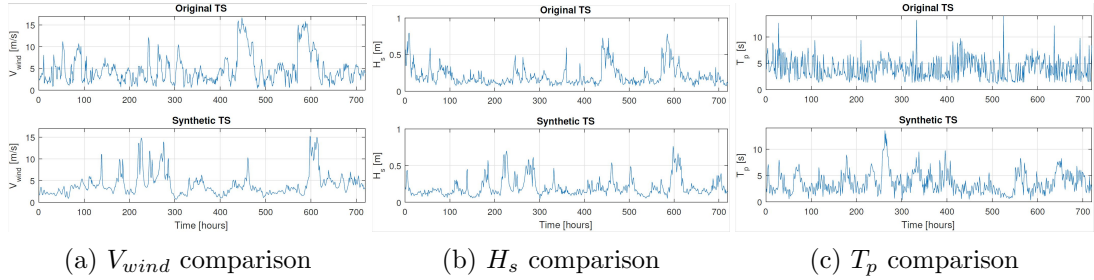


Figure 7. Synthetic - Original dataset comparison

Table 5. Comparison of statistical measures

V_{wind} (m/s)		Original				Synthetic					
		H_s (m)		T_p (s)		V_{wind} (m/s)		H_s (m)		T_p (s)	
μV_w	σV_w	μH_s	σH_s	μT_p	σT_p	μV_w	σV_w	μH_s	σH_s	μT_p	σT_p
4.53	3.12	0.193	0.123	3.94	1.89	4.525	3.16	0.19	0.122	3.89	1.9

However, for offshore installation and maintenance activities the duration of the operational windows is crucial. Therefore the synthetic time series were also validated in terms of the operational window persistence. This validation is based on a comparison of the cumulative distributions of the length of operational windows in the original and synthetic time series. This approach has also been used in a similar study (Leontaris et al., 2016), that concerns the modelling of dependence between wind velocity and significant wave height.

For validation purposes, the operational window persistence is observed for an offshore activity with the following arbitrary operating limits:

- H_s limit: 2.0 m
- V_{wind} limit: 7.0 m/s
- V_{curr} limit: 2.5 m/s

Figure 8 shows the cumulative distribution functions of the persistence for 1000 simulated time series, using the newly developed algorithm, and compares it with the operational window persistence in the original time series. It can be observed that the results from the synthetic time series are well clustered around the original time series. This is a strong indication that the synthetic time series have similar characteristics to the original data set, whilst including randomness to represent the environmental uncertainty.

Therefore, it can be concluded that the developed algorithm for simulating synthetic time series with both multivariate dependence and time dependence can be effectively implemented in offshore infrastructure planning models, as these show a strong resemblance to the operational window persistence of the original time series.

Additional validation has been performed in which the operational limits were adjusted. Due to the recurring character of the tidal current, the maximum operational window is strongly bounded by the V_{curr} limit. Still, when increasing the V_{curr} limit,

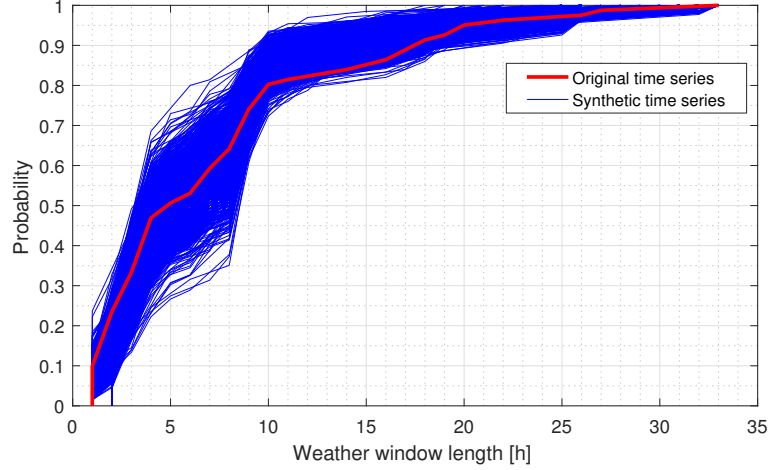


Figure 8. Comparison of the CDF of the persistence in the original and synthetic time series ($N_{sim} = 1000$)

it was observed that the operational window persistence showed a similar shape as in Figure 8, albeit with longer operational window lengths in the upper tail, depicted in Appendix D. So, the multivariate dependence is of added value for offshore infrastructure planning models, because the operational windows for different operations may vary substantially. To further investigate the synthetic time series, the persistence of the synthetic time series was also calculated and compared to the persistence of the original data set, when only one environmental variable is considered at a time. Figure 9 presents the persistence of the synthetic time series and that of the original dataset when considering the following environmental limits: $V_{wind} < 7m/s$ in Figure 9a, $H_s < 0.3m$ in Figure 9b and $T_p < 7s$ in Figure 9c. It can be seen that the persistence of synthetic time series are clustered around the persistence of the original dataset. This was expected since more possible weather realizations are taken into account.

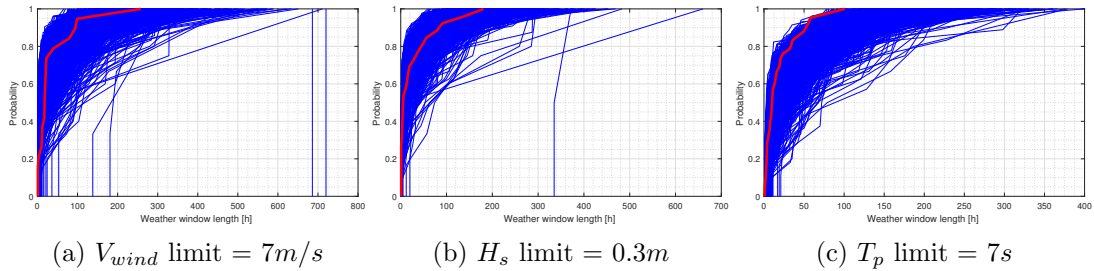


Figure 9. CDF of the weather windows' persistence when only one environmental variable is considered, in the original and synthetic time series ($N_{sim} = 1000$)

4. Replacement maintenance of tidal energy infrastructures

The management of maintenance of infrastructures (Crespo Márquez, 2007) can be split in two main processes, the definition of the strategy and the implementation of the strategy, often referred to as the maintenance policy. This should answer the ques-

tion of what activities should be performed, by whom and with what intention. In the case of early stage technology, such as tidal energy infrastructure, there is lack of operational experience (Strategic Initiative for Ocean Energy, 2013; Magagna & Uihlein, 2015), that introduces an uncertainty about the frequency and cost of maintenance interventions. Therefore, despite the numerous existing maintenance strategies, it is key to first use optimized corrective strategies to obtain operational insight, before moving on to complex preventive strategies which may require extensive knowledge of the tidal energy infrastructure.

In the past, tidal maintenance models have been developed (Y. Li & Florig, 2006) or are derived from the offshore wind industry (Mérigaud & Ringwood, 2016) to predict the overall maintenance costs, but little research has been done on the policy optimization of corrective maintenance models. Generic policy optimization models (Okumoto & Elsayed, 1983; Popova & Wilson, 1999; Assaf & Shanthikumar, 1987) can be applied, but these cannot describe the environmental uncertainty and cannot realistically describe the equipment failures and maintenance activities due to the large number of simplifications to be made to be able to solve it analytically.

At this point, it should be mentioned that one could also apply alternative approaches to solve the problem at hand. First, environmental conditions can be described by the use of Markov chains as presented in (Anastasiou & Tsekos, 1996). However, using discrete states for continuous variables might result in inaccuracies. Second, an alternative approach could be to use Markov theory again in order to describe the workable conditions. This approach translates the combination of environmental conditions into binary states (i.e workable and non-workable) which are also usually represented by Markov chains. In this case, using discrete binary sea states to describe a set of continuous variables, may again lead to inaccuracies. Moreover, this approach can quickly prove inefficient when more activities with different environmental limits are considered. Of course there are ways of dealing with this problem, but then the complexity of the model will increase with the number of operations with different limits. These approaches can be effective for scheduling of offshore operations, however there are the aforementioned limitations. The proposed approach using vine copulas overcomes these obstacles.

Therefore, this case study describes a methodology to reduce the cost of corrective maintenance of tidal energy infrastructures by assisting in optimal decision making. The developed model is applied to a tidal energy infrastructure concept by Damen Shipyards and uses environmental measurement data from FORCE, a tidal hotspot in Canada. The developed decision support tool enables the simulation of environmental time series with uncertainty and calculates whether a maintenance activity should be initiated for any of the tidal energy infrastructure's unique failure combinations in order to minimize the total cost of maintenance. The implemented maintenance strategy therefore describes the replacement of one or multiple failed Tidal Energy Converters (TECs) in the tidal energy infrastructure.

4.1. Tidal energy infrastructure description

The conceptual tidal energy platform developed by Damen Shipyards is visualized in Figure 10 and is used in this case study with the properties listed in Table 6. It consists of multiple Darrieus type TECs per tidal platform, which can each operate

and fail independently. Hence, failure of a TEC does not directly affect the others, except for when maintenance is to be performed. The entire platform is then emerged to the water surface after which failed TEC(s) can be replaced. A process flow of the individual vessel related tasks has been developed for describing the maintenance activity, as is seen in Figure 11.

Table 6. Maintenance model parameters

Tidal energy infrastructure		
Nr of platforms	$N_{platform}$	5
Nr of TECs/platform	N_{TEC}	16
TEC rated power	P_{rated}	110 kW
Feed-in Tariff	FiT	0.11 €/kWh
TEC failure		
TEC failure rate [†]	λ_{TEC}	0.29 year^{-1}
TEC replacement cost	C_{TEC}	$\text{€}104 \cdot 10^2$
Maintenance vessel		
TEC capacity of vessel	$N_{TEC,vessel}$	3

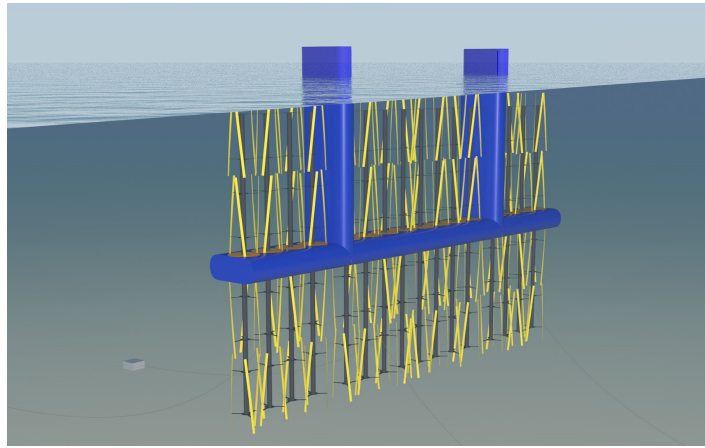


Figure 10. Concept design of the Damen tidal energy platform

In Figure 11 several loops can be observed. Based on the conditions of the maintenance activity and the tidal array, these loops are initiated. The loops describe the following:

- Loop A** More than one TEC is loaded, since multiple failed TECs will be replaced at once.
- Loop B** Multiple failed TECs at the same tidal platform will be replaced sequentially.
- Loop C** Failed TEC(s) at another platform will be replaced if the vessel still has TECs left.
- Loop D** More than one failed TEC has been replaced and is sequentially unloaded at the port.

[†]No data is available on tidal assembly failure rates, so reference values from offshore wind turbines are applied (Yu, Starke, Tolbert, & Ozpineci, 2007; Pudjianto et al., 2007; Arabian-Hoseynabadi, Oraee, & Tavner, 2010). The TEC failure rate is composed by including the following assemblies: Blades, generator, brake, gearbox, shaft and convertor.

Loop E The maintenance activity requires more TECs to be replaced than the vessel's deck capacity.

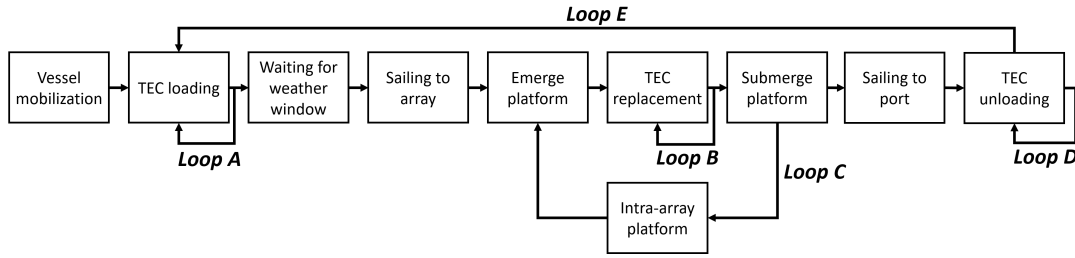


Figure 11. Process flow diagram of the maintenance vessel

For a safe and successful execution of a number of tasks a weather window is required since operational limits apply, which are dependent on the harshness of the weather conditions.

The included operational limits are determined by three criteria, namely:

Limit 1 Vessel sea-keeping performance.

Limit 2 Vessel station-keeping by using Dynamic Positioning when interacting with the tidal platform.

Limit 3 Motions of the vessel and tidal platform during the TEC lifting operation.

The task durations and operational limits are listed in Appendix B and have been determined by using expert judgments from Damen Shipyards.

4.2. Replacement maintenance model

The model which has been developed consists of two main processes, namely the generation of environmental time series with multivariate dependence and the optimization of the corrective maintenance policy maintenance. In Figure 12 the model's main framework is visualized.

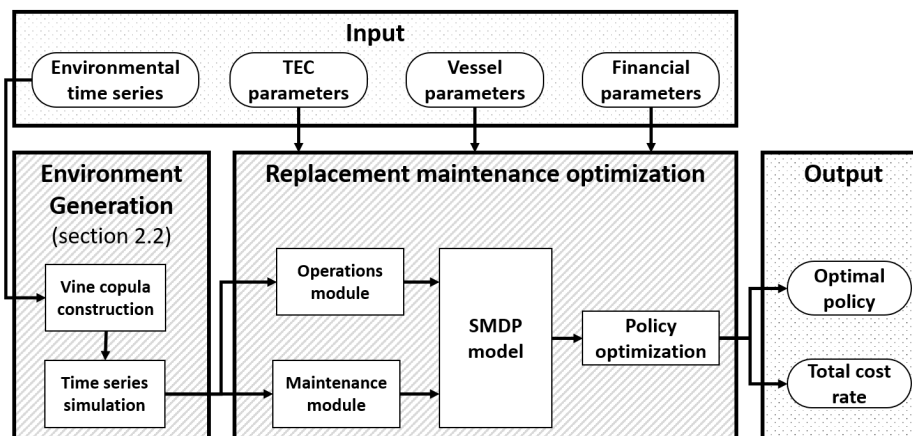


Figure 12. Model framework

The corrective maintenance model is run with 1000 generated synthetic time series, which are simulated by using the method described in section 2.2. It has been assumed that the number of simulations is large enough to represent any possible random occurrence of sea states. This implies that this probabilistic approach fully describes the uncertainty that is introduced by the randomness of the environmental conditions and therefore introduces the uncertainty of operational window in the model.

The collection of all possible maintenance decisions in the tidal energy infrastructure are described in a semi-Markov decision process (SMDP), first introduced by (Jewell, 1963) and (Cani, 1964) and also discussed in (Grabski, 2015). For a SMDP the optimal stationary policy with maximum gain can be found by applying the Howard algorithm (Howard, 1971; Mine & Osaki, 1971). The gain is the average reward per unit of time for the entire system. An infinite horizon SMDP with finite state and action spaces is considered, which satisfies the Markov property (or memoryless property) and implies that the conditional probability distribution of future states depend only on the present state of the system. This SMDP variant is known as a decision problem without discounting (Grabski, 2015). Several studies have previously used the SMDP approach with infinite horizon to optimize maintenance planning problems and minimize the total cost rate (Tijms, 2003; Tomasevicz & Asgarpoor, 2009). This approach requires the tidal energy infrastructure to be represented as summarized below. A detailed description of the SMDP model that was used for this case study can be found in Appendix C.

- **States** describe the unique combination of TEC failures in the array.
- **Decisions** describe whether or not maintenance is performed in each state, and how many TECs are to be replaced.
- **Transition probabilities** describing what the probability is of going from one state to another, based on the selected decision of performing maintenance (maintenance based transition) or doing nothing (failure based transition).
- **Transition rates** describe at what rate the transition from one state to another occurs. This is either induced by a TEC failure or the time it takes to perform maintenance.
- **Rewards** describe the benefits and costs of being in a particular state. This is directly related to downtime of one or more TECs and the cost of performing maintenance.

The optimal policy of the system describes the most economical decision to make in each state. For each of the tidal energy infrastructure’s unique failure combinations, the following questions are answered by the model:

- Should a maintenance operation be initiated?
- If so, how many TECs should be replaced in one maintenance operation?

The optimization model also determines the system’s gain rate, which is interpreted as the reward rate, given that the optimal policy is executed. In this model the rewards are represented by the costs, so the model will attempt to minimize the maintenance cost rate for the tidal array. The generated maintenance cost rate includes all costs which are included in the model, namely:

- TEC downtime costs.
- TEC repair costs (characteristic TEC product costs).
- Maintenance vessel costs.

The SMDP optimization assumes an infinite horizon, so the cost rate can be multiplied with the duration of interest to calculate the total expenditure on the listed maintenance related costs. Naturally, the estimated cost rate is bounded by the aforementioned assumptions and additional costs may apply in reality.

4.3. Added value of using vine copula based environmental synthetic time series

A comparative analysis is performed to showcase the added value of using vine copulas to generate synthetic time series with environmental uncertainty. The results of the model using the exclusively original measurement data from FORCE are compared with the results using the synthetic time series, which have been generated using vine copulas. This analysis compares the probabilistic maintenance activity duration for replacing an arbitrary number of TECs. This is directly influenced by the weather window uncertainty, which is induced by the interaction between the vessel's operational limits and the used environmental time series. For each analysis only the maintenance activity durations of replacing 1, 6 and 10 TECs are depicted in this section.

The first analysis compares the original and synthetic time series for a fixed starting point for the V_{curr} time series in order to determine what the influence is of generating more realizations to introduce uncertainty.

Figure 13 shows the activity durations for using the original and synthetic time series. The weather window limits have been selected to fully correspond to the base case, mentioned in section 4.2. Only one simulation can be run with the original time series data, so this results in a deterministic value, displayed by the red vertical line.

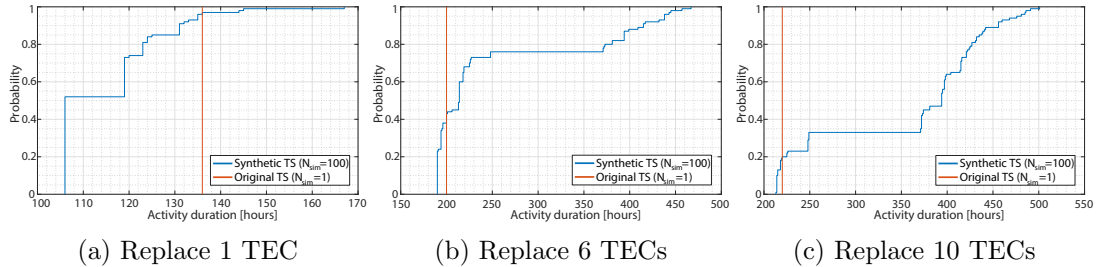


Figure 13. Comparison of activity duration with original and synthetic time series (fixed starting point)

It can be noted that, whilst keeping the current velocity time series fixed in all the simulations, still a large weather window uncertainty is introduced by applying the vine copulas to simulate synthetic time series for the H_s , T_p and V_{wind} variables. It is exactly this environmental randomness which can be included by simulating additional time series. Each of these synthetic time series add more possible environmental realizations, resulting in a probabilistic representation of the maintenance activity durations.

The second analysis enables multiple varying starting points in both the original and synthetic time series. This enables multiple simulations to be extracted from the same original time series in order to compare the probabilistic results of an approach without (original TS) and with vine copulas (synthetic TS).

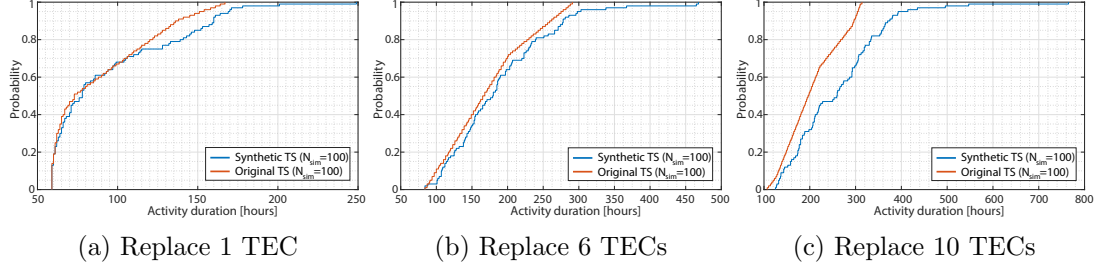


Figure 14. Comparison of activity duration with original and synthetic time series (variable starting point)

By using the original time series with a varying starting point, it is possible to construct different time series. However, a major limitation of this approach is its restriction in generating more environmental realizations than already exists in the original measurement data. Hence, it is not possible to describe the operational window uncertainty. It can be seen in Figure 14 that as the number of tasks increases, and thus the overall operational window length, the two approaches start showing a significant discrepancy.

On the other hand, by using a vine copula approach, it is possible to simulate as many synthetic time series as desired. This is a significant added value as more environmental realizations result in a more complete description of the weather induced uncertainty. Figure 14c illustrates a considerable underestimation of the activity duration, in case of using the original dataset instead of the synthetic time series ($\Delta T \approx 75$ hours at P90 value).

4.4. Replacement maintenance results

For each of the synthetic time series an optimal policy and corresponding replacement maintenance cost rate is calculated. The full set of identified cost rates can best be interpreted as the theoretical lower limit for performing replacement maintenance, given that the weather forecast is fully known for the decision maker at any moment in time. This should, theoretically, provide the required information to always select the best decisions for that specific state, given the full insight in the weather conditions for the time span of all possible activities.

Each of these identified optimal policies is the best policy to implement in that single simulation and has its own corresponding replacement maintenance cost rate. The cumulative distribution of the replacement maintenance cost rates is depicted in Figure 15 and represents the absolute minimum cost rate distribution of the tidal energy infrastructure.

In reality it is most common to operate by means of fixed decision rules, namely the recommended corrective maintenance policy. These dictate what decision should be taken in each state, without having full insights in the upcoming weather conditions. This requires us to narrow down the set of identified optimal policies to one recommended policy, which is an approximation of the theoretical lower limit and minimizes the corrective maintenance cost rate difference, based on a desired confidence level.

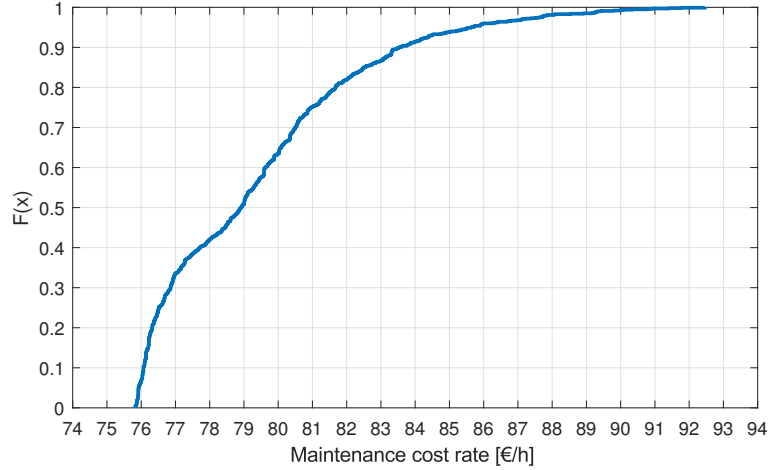


Figure 15. CDF of the minimum cost rate distribution (FORCE)

It should be noted that the selection of the confidence level is entirely up to the decision maker and the output of this decision support method can assist in gaining insight into the risks and gains which are related to different confidence levels. In total 155 unique policies have been found to represent the maintenance optima for different simulations. All the policies which occurred less than ten percent of the total simulations have been neglected and will be excluded in the policy analysis, resulting in policy A ($\approx 47\%$ occurrence) and policy B ($\approx 11\%$ occurrence).

To quantify the difference in terms of corrective maintenance cost rates, the policies A and B are plugged into the corrective maintenance model to execute its fixed set of decisions for each of the synthetic time series. Under the assumption that all environmental uncertainty is fully described, this results in the effective corrective maintenance cost rate distribution per fixed policy. The cost rate distributions of the two policies are also depicted in Figure 16. It can be seen that both policies result in distributions at nearly the same cost rates (i.e. ≈ 1 €/h at P90 value). Hence, these policies can be characterized as near-optimal.

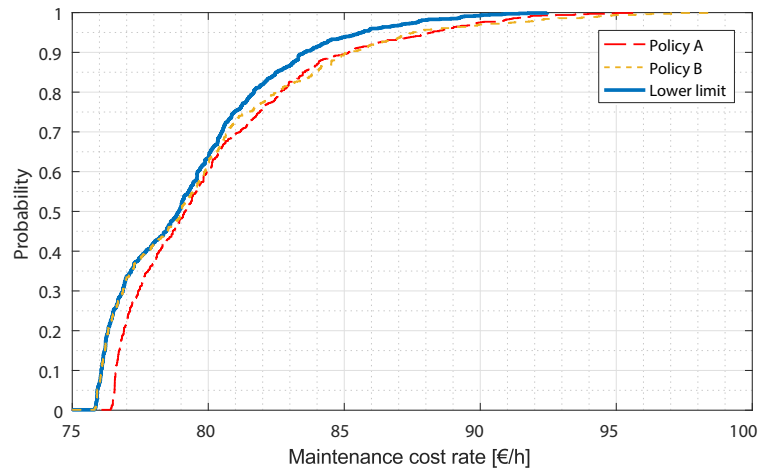


Figure 16. CDF of the minimum cost rate of the quasi-optimal policies A and B (FORCE)

5. Conclusions

In this article a method is proposed that uses vine copulas to construct time series of the dependent environmental conditions wind velocity, significant wave height, peak wave period and current velocity for a specific location of interest. These synthetic time series can support decision making processes for offshore infrastructure planning. It was shown that it is possible to generate synthetic time series that incorporate these dependencies. It also provides more possible realizations of the environmental conditions while the persistence of the operational windows remains comparable to the original limited dataset. In this way, it is possible to incorporate the dependent uncertainties of the offshore environmental conditions into the decision making processes.

To illustrate the impact in decision making, a replacement maintenance application case concerning a Tidal Energy Converter concept from Damen Shipyards for a specific tidal location in Canada was examined. A decision support tool has been developed based on a semi-Markov decision process, which uses the environmental time series and TEC parameters as input to determine optimal replacement maintenance policy. This policy describes what should be the combination of failed TECs for replacement maintenance to be initiated by a vessel, ensuring an overall cost minimization of both maintenance costs and revenue losses. The decision support tool enables the formal description of multiple failing components in the array, spread over several independent tidal platforms, and can therefore identify, for a particular environmental time series, an optimal replacement maintenance policy based on detailed failure combinations.

In order to investigate the impact of using vine copula based synthetic time series, the durations of certain activities were calculated and compared to the case where a the limited dataset was used. As it was expected, this limiting approach underestimated the duration of the activities because it did not take into account more possible realizations of the environmental conditions. Particularly, it is interesting to note that the limiting approach leads to a considerable underestimation of the operational windows and maintenance replacements, compared to the case where vine copulas were used to generate time series (underestimation percentage even up to $\approx 20\%$ in our case).

Additionally, when running the replacement maintenance model for each of the generated environmental time series, a probabilistic description of the cost rate of the optimal policy can be identified, which is based on the uncertainty of the occurring environmental conditions. Since there is a different optimal replacement policy for every synthetic time series, it is difficult for the decision maker to decide which one should be followed. Therefore, the two most occurring policies were simulated for the set of the synthetic time series and resulted in near-optimal cost rates. It should be noted that the cost rates of these near-optimal replacement policies had insignificant differences compared to the theoretical optimal ($\approx 1 \text{ €/h}$ at P90 value). Hence, these can be of assistance to practitioners who would be able to choose one particular replacement policy to plan the maintenance activities.

References

- Aas, K., & Berg, D. (2009). Models for construction of multivariate dependence - a comparison study. *European Journal of Finance*, 15(7-8), 639–659.
- Aas, K., Czado, C., Frigessi, A., & Bakken, H. (2009). Pair-copula constructions of multiple dependence. *Insurance: Mathematics and Economics*, 44(2), 182–198.
- Akaike, H. (1973). Information theory and an extension of the maximum likelihood principle. In *International symposium on information theory* (pp. 267–281).
- Anastasiou, K., & Tsekos, C. (1996). Operability analysis of marine projects based on Markov theory. *Applied Ocean Research*, 18(6), 329–352.
- Arabian-Hoseynabadi, H., Oraee, H., & Tavner, P. J. (2010). Failure modes and effects analysis (FMEA) for wind turbines. *International Journal of Electrical Power and Energy Systems*, 32(7), 817–824.
- Assaf, D., & Shanthikumar, J. G. (1987). Optimal group maintenance policies with continuous and periodic inspections. *Management Science*, 33(11), 1440–1452.
- Attoh-Okine, N. O. (2013). Pair-copulas in infrastructure multivariate dependence modeling. *Construction and Building Materials*, 49, 903–911.
- Bedford, T., & Cooke, R. M. (2001). Probability density decomposition for conditionally dependent random variables modeled by vines. *Annals of Mathematics and Artificial Intelligence*, 32(1-4), 245–268.
- Bedford, T., & Cooke, R. M. (2002, aug). Vines - A new graphical model for dependent random variables. *Annals of Statistics*, 30(4), 1031–1068.
- Cani, J. S. D. E. (1964). A dynamic programming algorithm for embedded Markov chains when the planning horizon is at infinity. *Management Science*.
- Clemen, R. T., & Reilly, T. (1999). Correlations and Copulas for Decision and Risk Analysis. *Management Science*, 45(2), 208–224.
- Crespo Márquez, A. (2007). *The maintenance management framework*. London: Springer London.
- Ellabban, O., Abu-Rub, H., & Blaabjerg, F. (2014). *Renewable energy resources: Current status, future prospects and their enabling technology* (Vol. 39).
- Embrechts, P., Lindskog, F., & Mcneil, A. (2003). Modelling dependence with copulas and applications to risk management. In *Handbook of heavy tailed distributions in finance* (pp. 329–384). Elsevier.
- Genest, C., & Favre, A.-C. (2007). Everything you always wanted to know about copula modeling but were afraid to ask. *Journal of Hydrologic Engineering*, 12(4), 347–368.
- Genest, C., Quessy, J. F., & Rémillard, B. (2006). Goodness-of-fit procedures for copula models based on the probability integral transformation. *Scandinavian Journal of Statistics*, 33(2), 337–366.
- Grabski, F. (2015). Ch. 15: Semi-Markov decision processes. *Semi-Markov Processes: Applications in System Reliability and Maintenance*, 229–244.

- Howard, R. A. (1971). *Dynamic probabilistic systems*. Wiley.
- Huang, W., & Prokhorov, A. (2014). A Goodness-of-fit test for copulas. *Econometric Reviews*, *33*(7), 751–771.
- International Renewable Energy Agency. (2014). *IRENA ocean energy technology brief 3* (Tech. Rep. No. June). Bonn: IRENA Innovation and Technology Centre.
- Jäger, W. S., & Nápoles, O. M. (2017). A vine-copula model for time series of significant wave heights and mean zero-crossing periods in the North Sea. *Journal of Risk and Uncertainty in Engineering Systems, Part A: Civil Engineering*, *3*(4), 1–25.
- Jewell, W. S. (1963). Markov-Renewal Programming. I: Formulation, Finite Return Models. *Operations Research*.
- Joe, H. (1996). Families of m-variate distributions with given margins and $m(m-1)/2$ bivariate dependence parameters. *Lecture Notes-Monograph Series*, *28*(1996), 120–141.
- Joe, H. (2015). *Dependence modeling with copulas*. Chapman and Hall/CRC.
- Joyce, J., Chang, N. B., Harji, R., & Ruppert, T. (2018). Coupling infrastructure resilience and flood risk assessment via copulas analyses for a coastal green-grey-blue drainage system under extreme weather events. *Environmental Modelling and Software*, *100*, 82–103.
- Kikuchi, Y., Ishihara, T., Skamarock, W. C., Klemp, J. B., Dudhia, J., Gill, D. O., . . . Powers, J. G. (2009). Assessment of weather window for the construction of offshore power plants by using wind and wave simulations Validation of simulation for wave and wind. In *Mmab technical note* (Vol. 276194). Copenhagen.
- Lawrence, J., Kofoed-Hansen, H., & Chevalier, C. (2009). High-resolution metocean modelling at EMEC's (UK) marine energy test sites. In *8th european wave and tidal energy conference*.
- Leontaris, G., Morales-Nápoles, O., & Wolfert, A. R. M. (2016). Probabilistic scheduling of offshore operations using copula based environmental time series An application for cable installation management for offshore wind farms. *Ocean Engineering*, *125*, 328–341.
- Li, D. Q., Phoon, K. K., Wu, S. B., Chen, Y. F., & Zhou, C. B. (2013). Impact of translation approach for modelling correlated non-normal variables on parallel system reliability. *Structure and Infrastructure Engineering*, *9*(10), 969–982.
- Li, Y., & Florig, H. (2006). Modeling the operation and maintenance costs of a large scale tidal current turbine farm. In *Oceans 2006*. Boston: IEEE.
- Liu, W., Wu, X., Zhang, L., & Wang, Y. (2017, oct). Probabilistic analysis of tunneling-induced building safety assessment using a hybrid FE-copula model. *Structure and Infrastructure Engineering*, 1–17.
- Magagna, D., & Uihlein, A. (2015). Ocean energy development in Europe: Current status and future perspectives. *International Journal of Marine Energy*, *11*, 84–104.
- Martin, R., Lazakis, I., Barbouchi, S., & Johanning, L. (2015). Identification and

- quantification of important offshore wind operations and maintenance factors. In *European wind energy association (ewea) conference*.
- Masina, M., Lamberti, A., & Archetti, R. (2015). Coastal flooding: A copula based approach for estimating the joint probability of water levels and waves. *Coastal Engineering*, *97*, 37–52.
- Mérigaud, A., & Ringwood, J. V. (2016). *Condition-based maintenance methods for marine renewable energy* (Vol. 66).
- Mine, H., & Osaki, S. (1971). Markovian Decision Processes. *SIAM Review*, *13*(4), 585–586.
- Montes-Iturrizaga, R., & Heredia-Zavoni, E. (2016). Multivariate environmental contours using C-vine copulas. *Ocean Engineering*, *118*, 68–82.
- Nævestad, M. (2009). *Multivariate distributions through pair-copula construction: Theory and applications*. Master thesis, Norwegian University of Science and Technology.
- Nelsen, R. B. (2006). An Introduction to Copulas. In *Springer series in statistics* (Second ed.).
- Ocean Networks Canada. (2017). *Data search oceans 2.0: Bay of Fundy, Minas Passage*. Retrieved 2017-07-09, from <http://dmas.uvic.ca/DataSearch?location=MIN>
- Okumoto, K., & Elsayed, E. A. (1983). An optimum group maintenance policy. *Naval Research Logistics Quarterly*, *30*(4), 667–674.
- Patil (Desai) Sujay, S., Wagh, M., & Shinde, N. (2017). A Review on Floating Solar Photovoltaic Power Plants. *International Journal of Scientific & Engineering Research*, *8*(6), 789.
- Popova, E., & Wilson, J. G. (1999). Group replacement policies for parallel systems whose components have phase distributed failure times. *Annals of Operations Research*, *91*(September), 163–189.
- Pudjianto, D., Pudjianto, D., Ramsay, C., Ramsay, C., Strbac, G., & Strbac, G. (2007). Virtual power plant and system integration of distributed energy resources. *Renewable Power Generation, IET*, *1*(1), 10–16.
- R Core Team. (2016). *R: A language and environment for statistical computing*. Retrieved from <https://www.r-project.org/>
- Schepsmeier, U., Stoeber, J., Brechmann, E. C., Graeler, B., Nagler, T., & Erhardt, T. (2016). *VineCopula: Statistical inference of vine copulas*. Retrieved from <https://cran.r-project.org/package=VineCopula>
- Schwarz, G. (1978). Estimating the dimension of a model. *The Annals of Statistics*, *6*(2), 461–464.
- Sibuya, B. M. (1960). Bivariate extreme statistics. *the Institute of Statistical Mathematics*, *10*(1), 195–210.
- Sklar, A. (1959). Fonctions de répartition à n dimensions et leurs marges. *Publications de l'Institut Statistique de l'Université de Paris*, *8*, 229–231.

- Stålhane, M., Vefsnmo, H., Halvorsen-Weare, E. E., Hvattum, L. M., & Nonås, L. M. (2016). Vessel fleet optimization for maintenance operations at offshore wind farms under uncertainty. *Energy Procedia*, *94*, 357–366.
- Strategic Initiative for Ocean Energy. (2013). *Ocean energy: Cost of energy and cost reduction opportunities* (Tech. Rep. No. May). Brussels: Strategic Initiative for Ocean Energy (SI OCEAN).
- Tang, X. S., Li, D. Q., Rong, G., Phoon, K. K., & Zhou, C. B. (2013). Impact of copula selection on geotechnical reliability under incomplete probability information. *Computers and Geotechnics*, *49*, 264–278.
- Tang, X. S., Li, D. Q., Zhou, C. B., & Phoon, K. K. (2015). Copula-based approaches for evaluating slope reliability under incomplete probability information. *Structural Safety*, *52*(PA), 90–99.
- Tijms, H. C. (2003). Semi-Markov decision processes. In *A first course in stochastic models* (2nd ed., pp. 279–305). John Wiley & Sons Ltd.
- Tomasevicz, C. L., & Asgarpoor, S. (2009). Optimum maintenance policy using semi-Markov decision processes. *Electric Power Systems Research*, *79*(9), 1286–1291.
- U.S. Energy Information Administration. (2017). International Energy Outlook 2017. *International Energy Outlook, IEO2017*, 76.
- Yu, X., Starke, M. R., Tolbert, L. M., & Ozpineci, B. (2007). Fuel cell power conditioning for electric power applications : a summary. *IET Electric Power Applications*, *1*(5), 643–656.

Appendix A. EMEC environmental time series analysis

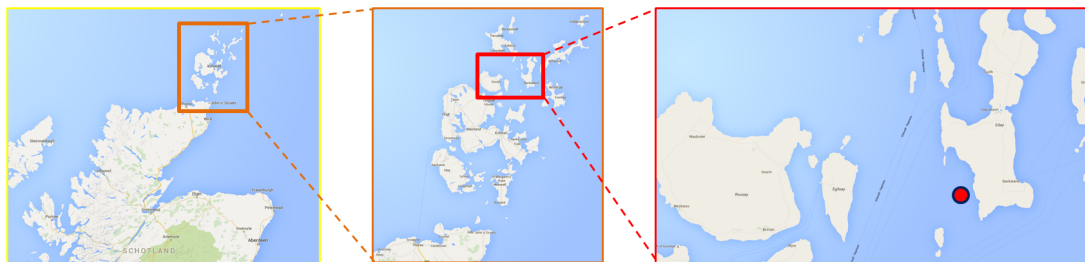


Figure A1. Geographical location of EMEC*

*Source: Google Maps

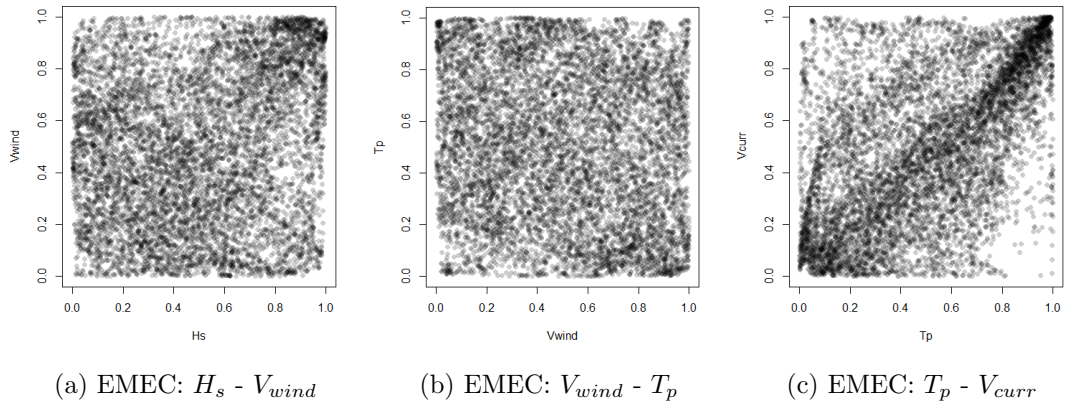


Figure A2. Scatter plots of EMEC pseudo-observations

A.1. Bivariate dependence

Table A1. Kendall's Tau rank correlations of EMEC data

	V_{wind}	H_s	T_p	V_{curr}
V_{wind}	1.000	0.121	-0.089	-0.003
H_s	0.121	1.000	0.077	-0.069
T_p	-0.089	0.077	1.000	0.394
V_{curr}	-0.003	-0.069	0.394	1.000

A.2. Base level factorisation

Table A2. Base level factorisation of EMEC data

	U_1	U_2	U_3	U_4
EMEC	V_{curr}	T_p	V_{wind}	H_s

A.3. Copula fitting and semi-correlations

Table A3. Semi-correlations and selected copula factorisation (EMEC)

Data set	ρ_{sw}	ρ_{total}	ρ_{ne}	Tail dependence	Copula
$V_{wind} - H_s$	-0.040	0.184	0.222	Upper	Gumbel
$H_s - T_p$	0.132	0.112	-0.010	Lower	Clayton
$T_p - V_{curr}$	0.271	0.546	0.400	Upper	Gumbel

Appendix B. Maintenance task durations and weather windows

Table B1. Required weather window of the maintenance operation

Task	Duration [hours]	Limit	Environmental limits			
			H_s [m]	T_p [s]	V_{wind} [m/s]	V_{curr} [m/s]
Vessel mobilization	24	-				
TEC loading	1	-				
TEC unloading	1	-				
Waiting for weather window	0*	-				
Sailing to array	2	1	2.5		9	
Sailing to port	2	1	2.5		9	
Intra-array transit	1*	1	2.5		9	
Emerge platform	2	2	2		7	2.5
Submerge platform	2	2	2		7	2.5
TEC replacement	1	3	1.5		6	2

* The mentioned duration is applied when no weather window related delays occur. This duration will therefore increase if waiting for a weather window of successive maintenance tasks is required.

Appendix C. Application of SMDP to the tidal system

C.1. SMDP representation

All system states and its transition properties (durations, probabilities and costs) are represented in a SMDP. A policy consists out of a set of actions per state and affects the transition properties, such as the ability to move from one state to another. For each policy the gain can be computed, which is the average reward per unit of time for the entire system. A policy iteration method, based on the Howard algorithm, can be used to identify improved policies with a higher gain compared to the initial policy. This process continues until the gain has converged to a maximum value, thus obtaining the optimized policy. Due to the nature of a SMDP (and its Markov property), the optimized policy of the SMDP therefore describes the best possible action per state, also taking into account all possible the effect of all future actions in the system.

C.2. States

Within this study the number of states has been linked to the number of unique failure combinations within the tidal array. Two types of states have been defined in the model to resemble the tidal energy infrastructure well:

- Deterioration states (D-states, S_D)
- Maintenance states (M-states, S_M)

Each deterioration state thus describes a unique combination of failed TECs within the array. This effectively enables the model to include all transitions and costs which occur if the system changes from one state to another, by either performing maintenance or wait for another TEC to fail. A simple serial example of the states and their

interaction is depicted in Figure C1a, in which the arrows indicate direction of state changes, red being a TEC failure, gray the decision of performing maintenance and green the replacement operation.

C.3. Decisions

It is important to note that, whilst the decisions have their own transition rates between states, the decision making moment is instantaneously upon entering the deterioration states from a previous state.

The primary decision set (D_x) can be chosen from any D-state:

Option 1 'Do Nothing' ($S_D \rightarrow S_D$)

Option 2 'Perform Corrective Maintenance' ($S_D \rightarrow S_M$)

If option 1 (D_1) is selected the system is left to deteriorate to a next state due to failure of an additional TEC. Selecting option 2 (D_2) initiates corrective maintenance and the corresponding maintenance state is entered in which the secondary decision has to be taken.

The secondary decision set ($D_{2,x}$) can be chosen from in any M-state:

Option 2.1 'Replace 1 TEC' ($S_M \rightarrow S_D$, with: $N_{TEC,fail,new} = N_{TEC,fail,old} - 1$)

Option 2.x 'Replace x TECs' ($S_M \rightarrow S_D$, with: $N_{TEC,fail,new} = N_{TEC,fail,old} - x$)

Due to the state architecture, this secondary decision set is only activated after the decision has been made to perform corrective maintenance (D_2) in a deterioration state. In the maintenance state it can be decided to replace a number of failed TECs, ranging between 1 and the number of failed TECs in the entire array, $N_{TEC,fail}$.

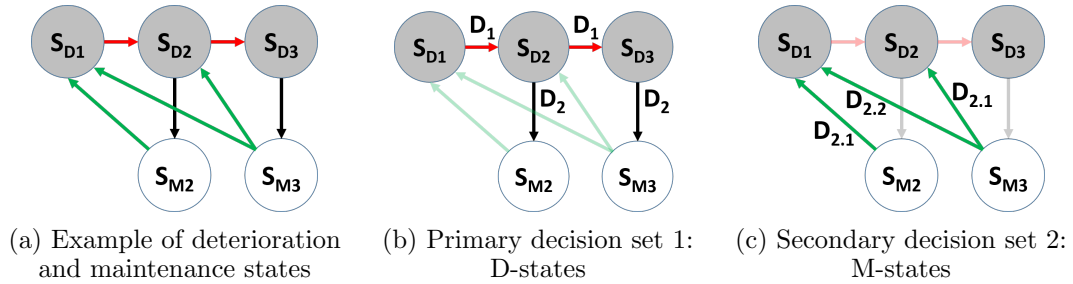


Figure C1. Decision sets for system states in SMDP representation

C.4. Deterioration module

In this section the methods will be explained to determine the transition rates, probabilities and rewards for the deterioration related process. This process is directly related to decision 1 (D_1 : 'Do Nothing'), so that the failures of TECs result in the transition from one deterioration state to another ($S_{D,from} \rightarrow S_{D,to}$), with increasing number of failed TECs ($N_{TEC,fail}$).

C.4.1. Failure transition probabilities

Transitions between the deterioration states do not necessarily have one predefined path, as the introduction of multiple platforms within the system allows multiple destination states in some cases.

For each deterioration state the transition probabilities of ending up in another deterioration state are calculated in a two-step process.

Step 1 Identify the deterioration states which have one more failed TEC than the departing state

$$(N_{TEC,fail,to} = N_{TEC,fail,from} + 1)$$

Step 2 Calculate the transition probabilities of going from the departing state ($S_{D,from}$) to the arrival state ($S_{D,to}$)

$$P_{S_{D,from} \rightarrow S_{D,to}} = \frac{N_{TEC,fail,pos,from \rightarrow to}}{N_{TEC,oper}} \quad (C1)$$

$$N_{TEC,oper} = N_{TEC,tot} - N_{TEC,fail} \quad (C2)$$

$$N_{TEC,fail} = \sum_{i=1}^{N_{platform}} N_{TEC,fail,i} \quad (C3)$$

It should be noted that the sum of all departing transition probabilities per decision adds up to one.

$$\sum_{i=1}^{N_{D,to}} P_{S_{D,from} \rightarrow S_{D,to,i}} = 1 \quad (C4)$$

C.4.2. Failure transition rates

In a SMDP all state transitions are represented as exponential distributions, which fully corresponds with the exponential distributions that describe the failure rate of a TEC. The following equation describes the transition rate for any arbitrarily deterioration state transition.

$$\lambda_{S_{D,from} \rightarrow S_{D,to}} = N_{TEC,fail,pos,from \rightarrow to} \cdot \lambda_{TEC} \quad (C5)$$

C.4.3. Production downtime costs ('Reward')

For decision 1, 'Do Nothing', the associated costs consist of the downtime costs, also defined as the indirect cost of maintenance ($E_{S_{D,from} \rightarrow S_{D,to}}$ in €). This is because a TEC failure results in a lack of electricity production. The downtime costs of a single

TEC is the net price of the electricity which would have been produced in the period of downtime, had the TEC not failed or undergoing maintenance.

The net amount of non-produced electricity during a state transition ($E_{S_{D,from} \rightarrow S_{D,to}}$ in kWh) is obtained by calculating the long term mean production ($P_{TEC,mean}$ in kWh) and then multiplying it with the number of failed TECs in the array ($N_{TEC,fail}$) and duration of the state transition, defined as the mean time between failure of the current state ($MTBF_{S_{D,from}}$ in years). The downtime cost ($C_{S_{D,from} \rightarrow S_{D,to}}$ in €) is then obtained by multiplying the net amount of non-produced electricity with the feed-in tariff (FiT in €/kWh) which applies to the tidal location. The equation to calculate these deterioration costs is as follows:

$$C_{S_{D,from} \rightarrow S_{D,to}} = E_{S_{D,from} \rightarrow S_{D,to}} \cdot FiT \quad (C6)$$

$$E_{S_{D,from} \rightarrow S_{D,to}} = N_{TEC,fail} \cdot P_{TEC,mean} \cdot (MTBF_{S_{D,from}} \cdot 365 \cdot 24) \quad (C7)$$

$$N_{TEC,fail} = \sum_{i=1}^{N_{platform}} N_{TEC,fail,i} \quad (C8)$$

$$MTBF_{S_{D,from}} = \frac{1}{\lambda_{S_{D,from}}} \quad (C9)$$

C.5. Maintenance module

Using a similar structure as the previous section, this section will present the methods to determine the transition rates, probabilities and rewards for the maintenance related process. This process is initiated when decision 2 (D_2 : 'Perform Maintenance') is selected in a state, after which the set of sub-decisions ($D_{2,x}$) determine how many TECs should be replaced at once.

The primary decision D_2 does not represent any physical process and imposes no costs ($C_{D2} = 0$). Upon selection of this primary decision, the state changes instantaneously ($T_{D2} = 0$) from the deterioration state to its corresponding maintenance state with probability one ($P_{D2} = 1$).

The transition rates, probabilities and rewards for the maintenance related process are thus exclusively related to the secondary decision set $D_{2,x}$.

C.5.1. Transition probabilities

This model allows a maximum of one TEC to fail during the execution of a maintenance activity of which the durations (T_{act}) are listed in appendix B. The chance of a TEC failure during the maintenance activity is

$$P_{TEC,fail} = \min\left(\frac{T_{act}}{(MTBF_{array} * 365 * 24)}, 1\right) \quad (C10)$$

$$MTBF_{array} = \frac{1}{\lambda_{array}} \quad (C11)$$

$$\lambda_{array} = N_{TEC,oper} \cdot \lambda_{TEC} \quad (C12)$$

with $MTBF_{array}$ being the failure time in years until one TEC fails in the array, given the current state.

Three characteristic situations may occur in the system:

- $T_{act} \ll (MTBF_{array} * 365 * 24) \rightarrow P_{TEC,fail} \approx 0$
This applies to most cases, since maintenance tasks usually last considerably shorter than the array failure time.
- $T_{act} \approx (MTBF_{array} * 365 * 24) \rightarrow P_{TEC,fail} \approx 1$
Especially in large arrays the $MTBF_{array}$ due to the large number of TECs. The failure probability increases as maintenance takes longer, or the time between TEC failure decreases.
- $T_{act} > (MTBF_{array} * 365 * 24) \rightarrow P_{TEC,fail} = 1$
If the maintenance activity duration exceeds that of the $MTBF_{array}$, it is assumed that a TEC will always fail during operation.

If $P_{TEC,fail}$ is calculated, the transition probabilities are calculated as follows:

$$P_{S_{M,from} \rightarrow S_{D,nofail}} = 1 - P_{TEC,fail} \quad (C13)$$

$$P_{S_{M,from} \rightarrow S_{D,fail,i}} = P_{TEC,fail} \cdot P_{S_{D,nofail} \rightarrow S_{D,fail,i}} \quad (C14)$$

The transition rate to the designated D-state without failure is $P_{S_{M,from} \rightarrow S_{D,nofail}}$, and the transition rate to any of the possible D-states when failure during the maintenance operation is described by $P_{S_{M,from} \rightarrow S_{D,fail,i}}$. The latter parameter uses the deterioration probabilities of the state that would have been arrived in, had failure not occurred.

C.5.2. Maintenance activity duration algorithm ('Transition rates')

The maintenance activity durations are calculated in a four step process, which is repeated N_{sim} times for each generated activity in the system.

- Step 1** Non-operable time steps per task are identified within the synthetic time series
- Step 2** All possible weather windows per task are calculated
- Step 3** The generated task sets per activity are sequentially projected onto the synthetic time series, attempting to fit the task on the first possible weather window after the final time step of the previous task

Step 4 The maintenance activity duration is the sum of all individual task durations ($T_{act} = \sum_{i=1}^{N_{task}} T_{task}$), including the intermediate periods of weather window waiting

Under the assumption that the calculated deterministic duration of the maintenance activities in hours is in fact the mean time to repair (MTTR) of the corresponding exponential maintenance activity duration distribution, the maintenance transition rates can be easily determined.

$$\lambda_{MTTR} = \frac{1}{MTTR} \quad (C15)$$

$$MTTR = T_{act} \quad (C16)$$

C.5.3. Maintenance costs ('Rewards')

The cost of executing a maintenance activity, and thus the costs when changing states due to the maintenance decision $D_{2,x}$, consists of three independent cost contributions, namely:

- Vessel activity costs
- TEC product costs
- Downtime costs

For an arbitrary maintenance operation the following holds:

$$C_{maint} = C_{act} + C_{TEC,tot} + C_{DT,tot} \quad (C17)$$

For each maintenance activity the individual task durations have been calculated per synthetic time series. To obtain the vessel maintenance costs, also referred to as the direct costs of maintenance, the task durations are to be multiplied with their respective cost rate.

$$C_{act} = \sum_{i=1}^{N_{task}} T_{task} \cdot C_{rate,task} \quad (C18)$$

The TEC product costs describe the mean repair costs of a TEC due to the 'as new' replacement of the failed assembly. 1

$$C_{TEC,tot} = C_{TEC} \cdot N_{TEC,repl} \quad (C19)$$

The downtime costs during the maintenance activity are calculated in a way similar to the one used for the deterioration related downtime costs.

Appendix D. Validation plots of synthetic time series

The observed task has the following operational limits:

- H_s limit: 2.0 m
- V_{wind} limit: 7.0 m/s
- V_{curr} limit: see Figure D1

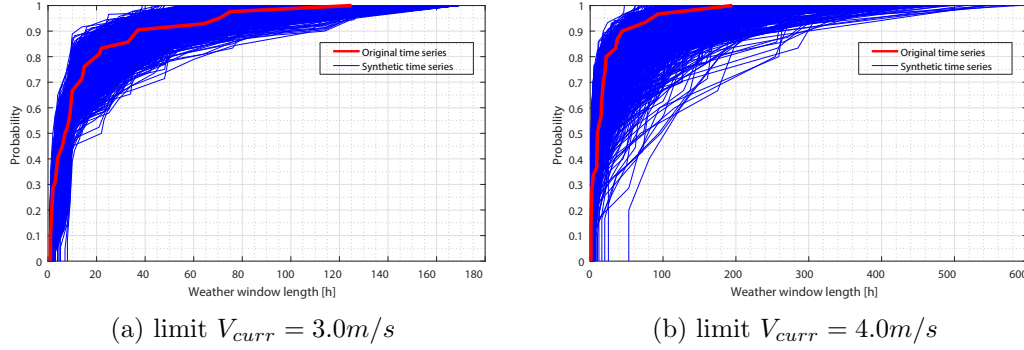


Figure D1. Comparison of the CDF of the persistence in the original and synthetic time series ($N_{sim} = 1000$) for different V_{curr} limits

Appendix E. Descriptive analysis of selected quasi-optimal maintenance policies

When comparing the two quasi-policies and their respective decisions per state, an interesting decision pattern was observed. It was found that three Decision Ranges (DRs) can be set up, which are related to the number of TEC failures ($N_{TEC,fail}$) of the respective states. The distribution of TEC failures among the tidal platforms does not affect these ranges.

The three DR which were identified in the analyzed optimal policies are:

- DR 1** Maintenance should never be performed.
- DR 2** Maintenance should be performed, based on the failure combination.
- DR 3** Maintenance should always be performed.

In DR 1 the replacement of the failed TECs never outweighs the cost due to the TEC downtime. The system is therefore left to deteriorate to subsequent D-states until the economical break-even point is achieved.

DR 2 can be seen as the transition between the D_1 ('Do Nothing') and D_2 ('Perform Corrective Maintenance') set of decisions. The two policies have very similar DR boundaries, but an unique set of decisions in DR 2. This shows that each of the two observed policies have near identical decisions and only differ slightly. It should be noted that for the two policies A and B the maximum number of TECs are replaced if decided to perform corrective maintenance.

All decisions in DR 3 are to perform corrective maintenance and replace $N_{TEC,fail}$, regardless of the failure combination. This can be explained by the physical repre-

sensation that the added cost of long maintenance activities (including sailing back and forth to the port to load more TECs) never becomes more expensive than the downtime costs of the non-replaced TEC(s). Also, the fixed mobilization costs of the vessel only have to be paid once when replacing all TECs in one maintenance activity.

The DR boundaries which apply to the two policies are shown in Table E1 and are defined by the number of failed TECs. These may be subjected to change when observing other policies or changing the system. The decisions per state of the two policies of DR 2 are visualized in Figure E1. The number of failed TECs per tidal platform in the array are listed in brackets left of each failure combination.

Table E1. Boundaries of the decision regimes for analyzed policies

DR	Lower boundary $[N_{TEC, fail}]$	Upper boundary $[N_{TEC, fail}]$
1	0	2 (3^*)
2	3 (4^*)	5
3	6	9

* the respective boundaries of policy A

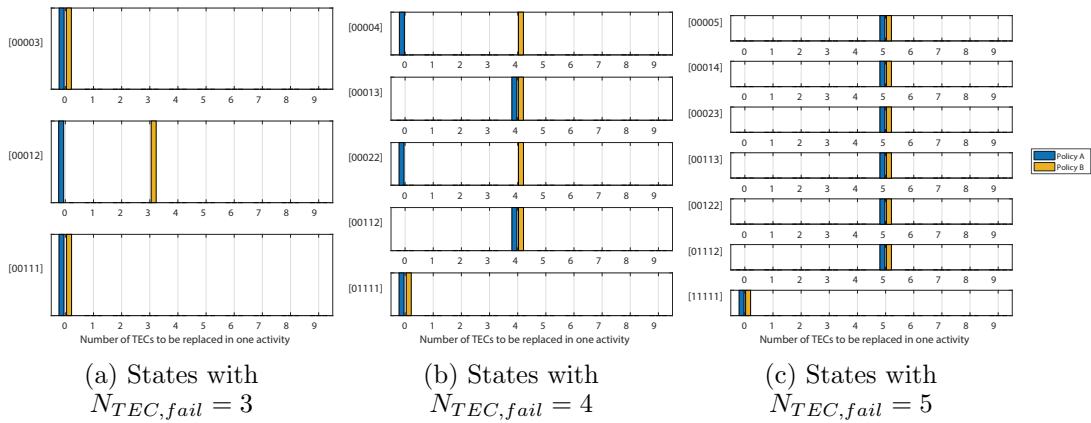


Figure E1. Decisions per state in DR 2 for the pseudo-optimal policies A and and C